Preparation and characterization of organo-functionalized silicas for bilirubin removal

UNIVERSITÀ DEGLI STUDI DI TORINO

Melusin protects from cardiac rupture and improves functional remodelling in mice after myocardial infarction

Bernhard Unsöld[1]*, Axel Kaul[1]*, Mauro Sbroggiò[2]*, Carola Schubert[3]*, Vera Regitz-Zagrosek[3], Mara Brancaccio[2], Federico Damilano[2], Emilio Hirsch[2] , Marc van Bilsen[4], Chantal Munts[4], Karin Sipido[5], Virginie Bito[5], Elke Detre[5], Nana Maria Wagner[1], Katrin Schäfer[1], Tim Seidler[1], Johannes Vogt[1], Stefan Neef[1],Annalen Bleckmann[6], Lars S. Maier[1], Jean Luc Balligand[7], Caroline Bouzin[7], René Ventura Clapier[8], Anne Garnier[8], Thomas Eschenhagen[9], Ali El-Armouche[10], Ralph Knöll[11], Guido Tarone[2§], and Gerd Hasenfuß[1§]

[1] Department of Cardiology, University of Göttingen, Heart Research Center Göttingen, Germany
[2] Department of Molecular Biotechnology and Health Sciences, University of Torino, Italy
[3] Institute of Gender in Medicine, Charité-Universitätsmedizin, Berlin, Germany
[4] Department of Physiology, Cardiovascular Research Institute Maastricht, Maastricht University, the Netherlands
[5]Division of Experimental Cardiology, Department of Cardiovascular Medicine, University of Leuven, Belgium
[6]Department of Hematology and Oncology, University of Göttingen, Germany
[7]Pharmacology and Therapeutics, Institut de Recherche Expérimentale et Clinique (IREC), Université catholique de Louvain, Brussels, Belgium
[8] INSERM U-769, Châtenay-Malabry, France
[9] Department of Experimental Pharmacology and Toxicology, University Medical Center Hamburg Eppendorf, Germany
[10]Department of Pharmacology, University of Göttingen, Heart Research Center Göttingen, Germany
[11] Myocardial Genetics, Imperial College London, United Kingdom

* the authors contributed equally to this work
§ the authors contributed equally to this work

Corresponding author:
Prof. Guido Tarone
Department of Molecular Biotechnology and Health Sciences
University of Torino
Italy
Phone: +39 0116706433
Fax: +39-0116706432
Email: guido.tarone@unito.it

Number of Words: 5712

ABSTRACT

Aims: Melusin is a muscle-specific chaperone protein whose expression is required for a compensatory hypertrophy response to pressure overload. Here we evaluated the consequences of melusin overexpression in the setting of myocardial infarction (MI) using a comprehensive multicenter approach.

Methods and Results:

Mice overexpressing melusin in the heart (TG) and wild type controls (WT) were subjected to permanent LAD-ligation and both the acute response (day 3) and subsequent remodelling (2 weeks) were examined. Mortality in wild type mice was significant between day 3 and 7, primarily due to cardiac rupture, but melusin overexpression strongly reduced mortality. At day 3 after MI, a timepoint preceding the mortality peak, TG hearts had increased Hsp70 expression, increased Erk1/2 signalling, reduced cardiomyocyte hyper-contractility and reduced inflammatory cell infiltrates in the infarcted area.

At 2 weeks after MI melusin overexpression conferred a favourable adaptive remodelling characterized by reduced left ventricle dilatation and better preserved contractility in presence of a comparable degree of hypertrophy. Adaptive remodelling in melusin TG mice was characterized by reduced apoptosis and fibrosis as well as increased cardiomyocyte contractility.

Conclusions: Consistent with its function as chaperone protein, Melusin overexpression exerts a dual protective action following MI reducing an array of maladaptive processes. In the early phase after MI, reduced inflammation and myocyte remodelling protect against cardiac rupture. Chronically, reduced myocyte loss and matrix remodelling, with preserved myocyte contractility, confer adaptive LV remodelling.

INTRODUCTION

Melusin is selectively expressed in skeletal muscle fibres and cardiomyocytes[1], and is required to activate a compensatory cardiac hypertrophy program in response to stress conditions such as chronic pressure overload of the left ventricle[2].

Melusin is endowed by chaperone activity as demonstrated by its ability to suppress the heat-induced protein denaturation[3] and binds the heat shock protein 90 (Hsp90), a major and well characterized chaperone protein. Melusin, by acting as an Hsp90 co-chaperone assists signaling proteins essential to trigger compensatory cardiomyocyte hypertrophy and survival such as AKT and Erks[2-7]. Melusin expression increases during the early phase of compensatory hypertrophy in mice subjected to aortic banding, while it decreases at later stages when the heart starts to dilate and contractile function declines[4]. In addition, in patients with heart failure secondary to aortic stenosis, the decline of systolic function is paralleled by a reduction of melusin expression[8], suggesting that high melusin expression levels are associated with better cardiac function under stress conditions. Indeed, forced melusin expression in the heart of transgenic mice protects against cardiac dilatation and failure allowing to maintain compensatory hypertrophy in response to long-standing pressure overload[4].

While the role of melusin has been studied in the setting of pressure overload induced hypertrophy[2,4] nothing is known so far about the role of melusin for the development of heart failure following myocardial infarction. Heart remodelling after myocardial infarction involves mechanisms different from those controlling hypertrophy in response to pressure overload. Indeed, coronary occlusion, causing lack of oxygen and metabolite supply, leads to acute tissue damage followed by the wound healing and scar formation. In parallel, the non-infarcted portion of the heart undergoes a deep remodelling to counteract the haemodynamic stress caused by the tissue loss. The efficacy of this remodelling has a major impact on the functional recovery and on the long-term survival[9-11]. In this study we used the model of permanent LAD ligation to investigate the impact of melusin over-expression on both the acute phase after MI and on the functional remodelling of the surviving myocardium.

The ability of chaperone proteins to mediate cytoprotective function requires pleiotropic action affecting several adaptive processes at the cellular and tissue level. These include assistance of protein folding, performing protein quality control, assembling of supra-molecular complexes and regulating signal transduction via different interconnected pathways. To gain a global view of pathways affected by melusin overexpression, we adopted a multicenter approach were each participating laboratory performed a specific intervention and/or analysis according to their specific expertise in a blinded way towards genotype and intervention. Although a large cohort of animals was examined, all interventions and statistical analyses were performed by blinded investigators at a core centre. This approach allowed maximal degree of standardization of the experimental

procedures and an unbiased analysis of the mouse phenotype. An array of potential mechanisms that could contribute to structural and functional remodelling after MI was analyzed, including i) stress proteins, ii) signalling effectors, iii) excitation-contraction coupling, iv) inflammatory responses, v) fibrosis, vi) apoptosis, and vii) expression of metabolic enzymes.

METHODS

Multicenter comprehensive matrix approach

To investigate the influence of genetic modifications in a comprehensive and systematic approach, a matrix was developed. The matrix allows parallel and unbiased investigation of an array of pathways exploiting the specific expertise within a European consortium of 21 partners (EUGeneHeart, supported by the EC under FP6).

At the core centre, all interventions were performed at a pre-specified age and weight of the animals by a single operator. In addition a single blinded investigator performed all echocardiographic analyses. At the time of sacrifice the hearts were harvested according to a standardized protocol. The samples were then processed and shipped to the partner laboratories to perform assays in the areas of their expertise. The technicians harvesting the hearts were blinded towards genotype and the type of intervention and the partner labs receiving the tissue samples for analysis were blinded towards sex, genotype and intervention performed.

Melusin overexpressing mice and animal experiments

Generation of FVB mice overexpressing human melusin (melusin-TG) has been described previously[4]. In brief the alpha-MHC promoter was cloned upstream the c-Myc-tagged human melusin cDNA followed by a beta-globin intron and a poly-A tail. The DNA construct was microinjected in FVB fertilized eggs and transgenic integration was confirmed by Southern blot.

Breeding pairs and the offspring used for the experiments were kept on an oestrogen free diet to allow for the analysis of gender effects without interference by exposure to phytoestrogens found in standard chow.

The investigation conforms to the Guide for the Care and Use of Laboratory Animals published by the US National Institutes of Health (NIH Publication No. 85-23, revised 1996). The experimental protocols were approved by the institutional review board of the University of Goettingen and the responsible government authority of Lower Saxony (Germany).

Induction of myocardial infarction

Mice aged 7-8 weeks were anaesthetised by isoflurane inhalation and endotracheally intubated. Anaesthesia was maintained by continuous inhalation of 1.5 % isoflurane in room air. Permanent ligation of the LAD immediately below the left atrial appendage was performed under isoflurane anaesthesia as detailed in the supplementary section. To

evaluate the extent of myocardial infarction, mice were anesthetized by IP injection of pentobarbital and heparin and hearts were quickly removed through a thoracotomy under full anaesthesia. The myocardium at risk was determined by coronary perfusion with Evan's blue and infarct size was determined by planimetry on tissue sections (see supplementary methods).

Echocardiography

Echocardiography was performed with a VisualSonicsVevo 660 system. 2D guided M-Mode echocardiography from the parasternal long-axis view was used to measure end-diastolic and end-systolic LV diameters and end-diastolic wall thickness. Fractional shortening was calculated as (LVEDD-LVESD)/LVEDD.

Autopsy study

To determine the cause of death after MI, a separate study comprising 31 male mice was performed. The mice were inspected three times daily until day 7 after induction of a myocardial infarction and were subjected to autopsy at the time of death. Cardiac tamponade or massive intra-thoracic hemorrhage were classified as signs for definite myocardial rupture. Presence of intra-thoracic blood led to classification as possible rupture.

Tissue harvesting and processing

At 3 days or 14±3 days after induction of a myocardial infarction, mice were anesthetized by IP injection of pentobarbital and heparin and the hearts were rapidly excised through a thoracotomy under full anaesthesia. The atria and adherent tissue were removed and heart weight was measured. A basal ring from the heart was sampled for histological analysis. In hearts subjected to myocardial infarction the scar was removed and the remaining tissue was frozen in liquid nitrogen. The frozen tissue was pulverized and aliquots were shipped to the participating laboratories for further analysis.

Histology

Myocyte cross sectional area was measured after WGA-staining. The number of phospho-Erk (p-Erk) positive nuclei 3 days after MI was determined by immunohistochemistry. TUNEL-staining was used for detection of apoptosis. The degree of fibrosis was determined by picrosirius red staining (see Supplementary methods).

mRNA quantification

mRNA transcript levels were determined by real-time quantitative PCR using SYBR-green after isolation and reverse transcription of mRNA according to standard procedures. The transcript levels were normalized for a housekeeping gene (see Supplementary methods).

Protein quantification

Western blotting was performed according to standard procedures (see Supplementary methods).

Calcium measurements

After isolation of single myocytes cell shortening was determined by edge tracking and intracellular calcium was measured by the calcium sensitive dye fluo-3 (see Supplementary methods).

Statistics

The data are presented as box plots representing median, interquartile range and minimum/maximum values as whiskers. For continuous data following a normal distribution differences between two groups were analysed by unpaired two-tailed Student's t-test; differences between more than two groups were analysed by one-way ANOVA with Bonferroni's post test. For data not following a normal distribution differences between two groups were analysed by a two-tailed Mann-Whitney test (indicated in the corresponding figure legend). Repeated measures were analysed by a two-way repeated measures ANOVA. Mortality rates were compared using the log-rank test. For the analysis of mortality peri-procedural deaths occurring within the first 24 hours after the operation were excluded. For western blot and real time data significant outliers were identified by the Grubb's outlier test and excluded from the analysis. A P-value <0.05 was considered statistically significant. In figures statistical significance is denoted by asterisks as follows *P<0.05, **P<0.01, ***P<0.001. GraphPad Prism 5.03 software was used for statistical analysis.

RESULTS

Melusin overexpression protects from cardiac rupture and mortality in the early phase following MI

To evaluate the potential effect of melusin overexpression, both infarct size and mortality were evaluated in WT and melusin-TG mice after MI.

Evan's Blue staining revealed that the volume of myocardium at risk did not differ between wild type and melusin-TG mice immediately after coronary artery ligation (*Figure 1A*) (44±2.5% vs. 41±3.3% of the LV mass, p=0.443 in wild type and melusin-TG respectively). Similarly the infarct size measured 3 days after ligation was not significantly affected by genotype (*Figure 1B*) (44.7±3.2% vs. 52.8±4.4%, p=0.139 in wild type and melusin-TG respectively).

Interestingly, however, mortality was significantly reduced in melusin-TG mice compared to wild type controls (*Figure 1C*) (43.2% vs. 27.3%, p=0.005 in wild type and melusin-TG respectively). Gender specific analysis showed that male wild type mice had a very high mortality after MI, compared to female mice (*Figure 1D, E*). Melusin overexpression strongly decreased mortality of male mice (*Figure 1D*) (63.1% vs. 40.6%, p=0.012 in wild type and melusin-TG respectively), but had a smaller effect, and did not reach statistical significance, in female mice (*Figure 1E*) (21.1% vs. 16%, p=0.422 in wild type and melusin-TG).

Kaplan-Meier curves indicate that the highest mortality occurred during the first week around day 5 after MI indicating a selective protective effect of melusin overexpression at this stage (*Figure 1C, D*). Autopsy of male mice having died during the first week after MI revealed that the majority of these mice showed signs of left ventricular rupture (*Figure 1F*). Histological analysis indicated loosened cardiomyocyte interactions and diffuse red blood cell and inflammatory cell infiltration (*Figure 1G*) strongly suggesting that melusin overexpression protects from cardiac rupture after MI.

Molecular and cellular events at 3 days after MI affected by Melusin overexpression.

Melusin is a chaperone protein and it is co-regulated with Hsp70[3], a major stress-induced protein acting as cytoprotective agent in response to a variety of different stress conditions including ischemia[12]. As shown in *Figure 2A* and *B*, both melusin and Hsp70 levels increased significantly 3 days after MI. Interestingly, Hsp70 level was higher in melusin-TG heart compared to WT in basal conditions (*Figure 2B*), confirming previous findings[3] and indicating that melusin-TG hearts possess a chaperone expression profile conferring a protective setting already in basal conditions.

Previous studies have shown that melusin enhances Erk1/2 signalling[4,5], a pathway well known for its protective function after MI[13]. As shown in *Figure 2C*, Erk phosphorylation in

cardiomyocytes at 3 days after MI was maximal in the border zone as detected by both phospho-Erk staining intensity and percentage of positive nuclei. Interestingly, melusin overexpression significantly potentiated this Erk phosphorylation (*Figure 2D, E*) suggesting a possible protective effect in melusin-TG mice.

Cardiomyocyte contractility undergoes important changes during post-MI remodelling with a phase of increased contractility followed by a late failing phase[14,15]. In line with previous studies, wild type cardiomyocytes isolated from hearts 3 days after MI showed faster contraction and relaxation than sham controls with larger Ca^{2+} transients (*Figure 2F and G*). Notably, this was not observed in melusin-TG mice (*Figure 2F and G*). In addition, 3 days after MI action potentials were significantly prolonged in wild type, but not in melusin-TG mice (not shown). Thus, melusin overexpression limits early phase calcium transients and cardiomyocyte hyper-contractility, likely reducing mechanical strain on the damaged left ventricle walls.

Inflammatory reaction plays an important role in the wound healing response in the early phase after MI[16,17]. We, thus, quantified the inflammatory cells in the infarcted zone at 3 days post MI. As shown in *Figure 3A*, infiltration of inflammatory cells was significantly reduced in melusin-TG compared to wild type mice. The infiltrating cells were mainly neutrophil granulocytes as judged by nuclear morphology (*Figure 3B*).

To better characterize the inflammatory pattern at 3 days post MI, we examined the expression levels of different cytokines, hypertrophic markers, and growth factors. While the levels of most of the markers examined were not significantly different in the infarcted hearts of wild type and melusin-TG mice (see supplementary material online, *Figure S1*), *Pgf* and *Cxcl10* were differentially regulated in the two mouse strains (*Figure 3C* and *D*). Interestingly, *Pgf, a* pro-angiogenic cytokine involved in reparative inflammatory reaction[18,19], was expressed at higher levels in melusin-TG hearts following MI. Moreover, the proinflammatory cytokine *Cxcl10* was expressed at lower levels in melusin-TG than wild type, consistently with the reduced number of infiltrating neutrophils.

At 3 days after MI, no significant effects of transgene-expression could be observed on the number of apoptotic cells or collagen deposition in the extracellular matrix (not shown).

In summary, melusin overexpression enhances Hsp70 levels and beneficial Erk1/2 signalling, it normalizes calcium handling and contractility and reduces inflammation in the ischemic zone, ultimately protecting male mice from cardiac rupture.

Melusin overexpression improves LV functional recovery after myocardial infarction

Having established a clear protective effect of melusin overexpression in the acute response to MI, we evaluated the possible impact of melusin overexpression on functional remodelling of remote myocardium after MI.

Cardiac hypertrophy, as measured by heart weight relative to body weight, was induced to a similar extent in melusin-TG and wild type mice at 2 weeks after MI (*Figure 4A*). Interestingly, however, melusin-TG hearts showed less dilatation (*Figure 4B*) and better preserved septal wall thickness (*Figure 4C*) compared to wild type animals. Moreover, contractile function, measured by fractional shortening, was better preserved in melusin-TG hearts at 2 weeks after MI (*Figure 4D*). At the cellular level significant myocyte hypertrophy could only be demonstrated in melusin-TG myocardium following MI (*Figure 4E*). Analysis of mRNA-expression of the atrial natriuretic factor (*Nppa*), as marker for heart failure, revealed a higher induction in wild type mice compared to melusin-TG (*Figure 4F*) confirming improved remodelling in these mice.

Melusin overexpression does not significantly alter metabolic enzyme expression.

A switch from fatty acid to glucose metabolism is accompanying the evolution toward heart failure[20]. Reduced expression of PPAR-alpha co-activator proteins like PGC-1-alpha as well as of *Acsl1* and *Hadha*, two enzymes involved in cardiac fatty acid metabolism, were significantly reduced in the heart of wild type mice 2 weeks post MI (supplementary material online, *Figure S2 C, E, F*). This drop in expression was not significant in melusin TG heart after MI, but the mRNA levels of these proteins tended to be lower in sham-operated melusin-TG mice than in WT. A number of other metabolic enzymes were also examined (supplementary material online, *Figure S2*) and since these differences were not statistically significant we conclude that alterations in metabolic enzyme expression unlikely impact on the favourable remodelling observed in TG mice.

Melusin overexpression improves cardiomyocyte contractility following myocardial infarction.

The partial preservation of LV contractile function in melusin-TG animals as detected by echocardiography (*Figure 4D*) might be explained by differences in myocyte function and excitation contraction coupling. To investigate whether melusin impacts on these parameters, isolated myocytes were investigated by simultaneous Ca^{2+} fluorescence and sarcomere length measurements. After MI the surviving cardiac myocytes of WT mice showed increased fractional shortening as illustrated in *Figure 5A* demonstrating a compensatory increase of inotropy. This effect was even more pronounced in melusin-TG animals following myocardial infarction with significantly higher myocyte fractional shortening (*Figure 5A*) ($p<0.05$ for wild type MI vs. melusin-TG MI), suggesting a beneficial effect of melusin on contractility in the surviving myocytes after myocardial infarction. Interestingly, Ca^{2+} transient amplitudes were unaltered following the intervention (not shown), suggesting that the increase in single cell contractility resulted from increased myofilament Ca^{2+} sensitivity. Consistent with unaltered calcium cycling, the expression levels

of SERCA2a (*Figure 5B*), calsequestrin and phospholamban (supplementary material online, *Figure S3*) were not influenced significantly by melusin overexpression or the presence of a myocardial infarction. At the same time, the finding that troponin Ser22/23 phosphorylation was reduced in WT, but not in melusin-TG hearts after MI (*Figure 5C*), supports the hypothesis of increased myofilament Ca^{2+} sensitivity and better contractility in melusin overexpressing mice.

Melusin overexpression decreases apoptosis and collagen deposition in the remote myocardium

Apoptotic death of cardiomyocytes and deposition of fibrotic tissue are major causes of unfavourable heart remodelling in different pathological conditions including MI. We therefore evaluated these parameters. The number of apoptotic cells in the remote myocardium, as assessed by TUNEL staining, was significantly lower in melusin-TG compared to wild type animals (*Figure 5D*), indicating a significant protection from apoptosis mediated by the transgene.

At the same time, collagen deposition in the remote myocardium, as assessed by picrosirius red staining, was significantly lower in melusin-TG animals than in wild type littermates after myocardial infarction (*Figure 5E*).

Overall these data indicate that overexpression of melusin favours an adaptive remodelling of the remote myocardium after MI mainly by increasing cardiomyocyte contractility and by reducing apoptotic death and fibrosis.

DISCUSSION

Using a multicenter collaborative approach we identified two major protective end-effects of transgenic melusin overexpression in the murine heart. First, melusin overexpression strongly reduces mortality in the acute phase after MI by protecting from myocardial rupture. Second, melusin overexpression reduces maladaptive remodelling of the remote myocardium.

The role of a gene on a given physio-pathological process is frequently investigated by focusing on the characterization of a specific mechanism or pathway proposed to be regulated by that gene. This approach allows a detailed understanding of the contribution of a given biochemical pathway to that particular phenotype. However, the concept of signalling networks that impact on a wide variety of different cellular functions is increasingly recognized[21]. In particular in the case of chaperone proteins such as melusin, multiple pathways are likely to be affected[22-23]. Therefore, a broad spectrum and unbiased analysis is required to gain a comprehensive view of the relevant mechanisms impacting on (mal)adaptive remodelling processes.

We have shown in this study that melusin is up-regulated in the remote myocardium after MI together with the Hsp70, another well characterized chaperone[24] indicating that both melusin and Hsp70 belong to the stress molecules upregulated after ischemia. Interestingly, melusin-TG hearts expressed higher levels of Hsp70 (*Figure 2B*) under unstressed conditions, implying that melusin overexpression drives increased expression of Hsp70. Hsp70 is known to exert protective functions after MI[25] and to possess anti-inflammatory activity[26-28]. High chaperone molecule expression confers a highly cytoprotective setting to melusin-TG hearts.

Chaperones, such as Hsp70 and Hsp90, promote protein folding through ATP-regulated cycles of binding and release. This chaperone machinery play a crucial role in signal transduction assisting the conformational switches occurring during activation and deactivation of signalling proteins[29]. We have previously shown that melusin, by organizing a supramolecular signalosome, involving chaperones, scaffolds and kinases molecules[5], promotes activation of the Erk1/2 cascade, a well known cardioprotective signalling pathway inducing cardiomyocyte hypertrophy and survival[5]. In line with these findings we showed that Erk1/2 phosphorylation was significantly increased in the border zone of the infarcted myocardium in melusin-TG mice. The border zone is a region of tissue subjected to the highest mechanical stretch immediately after MI. Increased Erk1/2 phosphorylation in melusin-TG hearts, thus, suggests a protective role in withstanding the tensile stress and reducing the incidence of cardiac rupture.

A further consequence of melusin induced cardiomyocyte protection from stress is represented by a reduced alteration in calcium handling and contractility after MI. In fact, we found faster contractions and increased calcium transient amplitudes following MI in wild type mice, as reported before[15], but not in melusin-TG male mice. This finding might reflect mitigation of the signals that lead to the early response after MI, likely through reduced inflammatory signals (see below). The slower twitch kinetics decrease strain in melusin-TG mice post MI and may, thus, decrease incidence of rupture.

Inflammatory infiltration is an additional important mechanism affecting cardiac rupture post-MI[30]. Our results indicate that melusin overexpression strongly reduce inflammatory infiltrates in the infarcted area in the early phase (3 days) after MI preceding the peak of death occurring around day 5 due to cardiac rupture. The reduced inflammatory reaction was also reflected by a peculiar pattern of inflammatory cytokines. In particular, melusin-TG infarcted hearts showed decreased expression of Cxcl10 and increased expression of Pgf. Cxcl10 is a well characterized inflammatory cytokine involved in recruiting leukocytes to inflamed tissues, perpetuating inflammation and causing tissue damage[31]. Pgf has been shown to exert a dual action as regulator of reparative inflammation[18] and as a pro-angiogenic factor via recruitment of endothelial progenitors[19]. Moreover, Pgf shows protective effects following MI in human patients[32] and in mouse models of heart failure[18,19]. Thus, the decreased level of Cxcl10 and increased level of Pgf in the acute response to MI correlate with the observed reduction of the inflammatory infiltrate and the ability of melusin to shift inflammation toward a reparative process.

While current therapeutic interventions allow an efficient and successful control of the acute MI, better treatments to prevent maladaptive functional remodelling and heart failure in the long term still need to be developed. In fact, compensatory remodelling of the remote zone after MI is a crucial event determining optimal functional recovery and favourable long term prognosis. The results reported in this work indicate an important contribution of melusin in sustaining functional remodelling in the two weeks after MI. In fact, while no differences were observed in the increase of relative heart weight between wild type and melusin-TG hearts, the left ventricles of melusin-TG animals were less dilated, contractility was better preserved and Anf levels were reduced compared to wild type mice. Improved functional remodelling in melusin overexpressing animals was likely due to increased hypertrophy and contractility of transgenic cardiomyocytes as well as to reduced apoptosis and fibrosis in the non-infarcted myocardium. The relevance of these parameters for the positive remodelling is further highlighted by the fact that metabolic enzyme levels and angiogenic response were not significantly altered by transgene expression.

In conclusion, Melusin overexpression exerts a dual protective action following MI reducing an array of maladaptive processes consistent with its chaperone function on multiple targets. In the early phase after MI, reduced inflammation and myocyte remodelling protect against cardiac rupture; chronically, reduced myocyte loss and matrix remodelling, with preserved myocyte contractility confer adaptive LV remodelling with improved cardiac function.

Acknowledgements

Expert technical assistance was provided by Patricia Holemans, Christel Huysmans (KULeuven), Antje Schneeberg, Jessica Spitalieri, Anke Rüttgeroth, Kirsten Koschel, Michael Kothe, Timo Schulte, Thomas Sowa (University of Göttingen), Jutta Starbatty, Thomas Schulze (University of Hamburg), Delphine De Mulder (UCLouvain). This work was supported by a EU FP6 grant LSHM-CT-2005-018833, EUGeneHeart.

REFERENCES

1. Brancaccio M, Guazzone S, Menini N, Sibona E, Hirsch E, De Andrea M*, et al.* Melusin is a new muscle-specific interactor for beta(1) integrin cytoplasmic domain. *J Biol Chem* 1999;**274**:29282-29288.
2. Brancaccio M, Fratta L, Notte A, Hirsch E, Poulet R, Guazzone S*, et al.* Melusin, a muscle-specific integrin beta1-interacting protein, is required to prevent cardiac failure in response to chronic pressure overload. *Nat Med* 2003;**9**:68-75.
3. Sbroggio M, Ferretti R, Percivalle E, Gutkowska M, Zylicz A, Michowski W*, et al.* The mammalian CHORD-containing protein melusin is a stress response protein interacting with Hsp90 and Sgt1. *FEBS Lett* 2008;**582**:1788-1794.
4. De Acetis M, Notte A, Accornero F, Selvetella G, Brancaccio M, Vecchione C*, et al.* Cardiac overexpression of melusin protects from dilated cardiomyopathy due to long-standing pressure overload. *Circ Res* 2005;**96**:1087-1094.
5. Sbroggio M, Bertero A, Velasco S, Fusella F, De Blasio E, Bahou WF*, et al.* Erk1/2 activation in heart is controlled by melusin, focal adhesion kinase and the scaffold protein IQGAP1. *J Cell Sci* 2011;**124**:3515-3524.
6. Ferretti R, Sbroggio M, Di Savino A, Fusella F, Bertero A, Michowski W*, et al.* Morgana and melusin: two fairies chaperoning signal transduction. *Cell Cycle* 2011;**10**:3678-3683.
7. Purcell NH, Wilkins BJ, York A, Saba-El-Leil MK, Meloche S, Robbins J*, et al.* Genetic inhibition of cardiac Erk1/2 promotes stress-induced apoptosis and heart failure but has no effect on hypertrophy in vivo. *Proc Natl Acad Sci U S A* 2007;**104**:14074-14079.
8. Brokat S, Thomas J, Herda LR, Knosalla C, Pregla R, Brancaccio M*, et al.* Altered melusin expression in the hearts of aortic stenosis patients. *Eur J Heart Fail* 2007;**9**:568-573.
9. Tiyyagura SR, Pinney SP. Left ventricular remodelling after myocardial infarction: Past, present and future. *Mount Sinai Journal of Medicine* 2006;**73**:840-851.
10. Opie LH, Commerford PJ, Gersh BJ, Pfeffer MA. Controversies in Cardiology 4 - Controversies in ventricular remodelling. *Lancet* 2006;**367**:356-367.
11. Pfeffer MA, Braunwald E. Ventricular Remodelling after Myocardial-Infarction - Experimental-Observations and Clinical Implications. *Circulation* 1990;**81**:1161-1172.
12. Willis MS, Patterson C. Hold me tight: Role of the heat shock protein family of chaperones in cardiac disease. *Circulation* 2010;**122**:1740-1751.
13. Yeh CC, Malhotra D, Yang YL, Xu Y, Fan Y, Li H*, et al.* MEK1-induced physiological hypertrophy inhibits chronic post-myocardial infarction remodelling in mice. *J Cell Biochem* 2013;**114**:47-55.
14. Mork HK, Sjaastad I, Sejersted OM, Louch WE. Slowing of cardiomyocyte Ca2+ release and contraction during heart failure progression in postinfarction mice. *Am J Physiol Heart Circ Physiol* 2009;**296**:H1069-1079.
15. Mork HK, Sjaastad I, Sande JB, Periasamy M, Sejersted OM, Louch WE. Increased cardiomyocyte function and Ca2+ transients in mice during early congestive heart failure. *J Mol Cell Cardiol* 2007;**43**:177-186.
16. Frangogiannis NG. Regulation of the inflammatory response in cardiac repair. *Circ Res* 2012;**110**:159-173.
17. Ertl G, Frantz S. Healing after myocardial infarction. *Cardiovasc Res* 2005;**66**:22-32.
18. Carnevale D, Cifelli G, Mascio G, Madonna M, Sbroggio M, Perrino C*, et al.* Placental growth factor regulates cardiac inflammation through the tissue inhibitor of metalloproteinases-3/tumor necrosis factor-alpha-converting enzyme axis: crucial role for adaptive cardiac remodelling during cardiac pressure overload. *Circulation* 2011;**124**:1337-1350.
19. Iwasaki H, Kawamoto A, Tjwa M, Horii M, Hayashi S, Oyamada A*, et al.* PlGF repairs myocardial ischemia through mechanisms of angiogenesis, cardioprotection and recruitment of myo-angiogenic competent marrow progenitors. *PLoS One* 2011;**6**:e24872.
20. Sack MN, Rader TA, Park S, Bastin J, McCune SA, Kelly DP. Fatty acid oxidation enzyme gene expression is downregulated in the failing heart. *Circulation* 1996;**94**:2837-2842.

21. Natarajan M, Lin KM, Hsueh RC, Sternweis PC, Ranganathan R. A global analysis of cross-talk in a mammalian cellular signalling network. *Nat Cell Biol* 2006;**8**:571-580.
22. Nair SC, Toran EJ, Rimerman RA, Hjermstad S, Smithgall TE, Smith DF. A pathway of multi-chaperone interactions common to diverse regulatory proteins: estrogen receptor, Fes tyrosine kinase, heat shock transcription factor Hsf1, and the aryl hydrocarbon receptor. *Cell Stress Chaperones* 1996;**1**:237-250.
23. Meimaridou E, Gooljar SB, Chapple JP. From hatching to dispatching: the multiple cellular roles of the Hsp70 molecular chaperone machinery. *J Mol Endocrinol* 2009;**42**:1-9.
24. Hartl FU, Bracher A, Hayer-Hartl M. Molecular chaperones in protein folding and proteostasis. *Nature* 2011;**475**:324-332.
25. Latchman DS. Heat shock proteins and cardiac protection. *Cardiovasc Res* 2001;**51**:637-646.
26. Jones Q, Voegeli TS, Li G, Chen Y, Currie RW. Heat shock proteins protect against ischemia and inflammation through multiple mechanisms. *Inflamm Allergy Drug Targets* 2011;**10**:247-259.
27. Borges TJ, Wieten L, van Herwijnen MJ, Broere F, van der Zee R, Bonorino C*, et al.* The anti-inflammatory mechanisms of Hsp70. *Front Immunol* 2012;**3**:95.
28. Ortega E, Bote ME, Besedovsky HO, del Rey A. Hsp72, inflammation, and aging: causes, consequences, and perspectives. *Ann N Y Acad Sci* 2012;**1261**:64-71.
29. Picard D. Chaperoning steroid hormone action. *Trends Endocrinol Metab* 2006;**17**:229-235.
30. Gao XM, White DA, Dart AM, Du XJ. Post-infarct cardiac rupture: recent insights on pathogenesis and therapeutic interventions. *Pharmacol Ther* 2012;**134**:156-179.
31. Lee EY, Lee ZH, Song YW. CXCL10 and autoimmune diseases. *Autoimmun Rev* 2009;**8**:379-383.
32. Iwama H, Uemura S, Naya N, Imagawa K, Takemoto Y, Asai O*, et al.* Cardiac expression of placental growth factor predicts the improvement of chronic phase left ventricular function in patients with acute myocardial infarction. *J Am Coll Cardiol* 2006;**47**:1559-1567.

FIGURE LEGENDS

Figure 1:

Melusin overexpression increases survival reducing cardiac rupture after MI.

(*A*) Following LAD-ligation wild type and melusin transgenic mice displayed a comparable volume at risk as detected by Evan's blue staining (44±2.5% in wild type vs. 41±3.3% in melusin-TG of the LV mass, P=0.443). (*B*) Similarly 3 days post MI infarct size was not significantly different in wild type animals and melusin-TG (44.7±3.2% in wild type vs. 52.8±4.4% in melusin-TG, P=0.139). (*C*) Kaplan-Meier analysis showed that mortality after MI was significantly decreased in melusin-TG animals (43.2% (n = 190) in wild type vs. 27.3%(n = 150) in melusin-TG, P=0.005). (*D*) Gender specific analysis showed that male wild type mice had a very high mortality which was strongly decreased by melusin overexpression (63.1% (n=100) in wild type vs. 40.6% (n=69) in melusin-TG, P=0.012). (E) Female mice showed a much lower mortality compared to male (*D*) and melusin overexpression further reduced mortality, even though not to a statistically significant value (21.1% (n=90) wild type vs. 16% in melusin-TG (n=81), P=0.422). (*F*) Autopsy of wild type mice having died during the first week after MI revealed that mortality was predominantly caused by myocardial rupture. (*G*) Histological sections from these mice displayed loosened cardiomyocyte interactions and diffuse red blood cell (arrows) and inflammatory cell infiltration.

Figure 2:

Expression of Melusin and Hsp70 increase after MI. (*A*) Western blot analysis showed increased levels of melusin expression in wild-type mice 3 days after MI (1.03 ± 0.035 in wild type sham vs. 2.56 ± 0.126 in wild type MI, P=0.007) (*B*) Hsp70 expression also increased in both WT and melusin-TG hearts following MI. Interestingly melusin-TG male mice showed increased Hsp70 protein expression under baseline conditions (1,22±0,054 in wild type sham vs. 3,48 ± 0,11 in melusin-TG sham, P=0,0002).

Melusin overexpression stimulates Erk1/2 signaling after MI (*C-E*). Low magnification picture of a melusin-TG mouse heart 3 days post MI stained with p-Erk antibodies without counterstaining (*C*). p-Erk reactivity is mostly confined to the border zone between the septum (remote area) and the free wall (infarcted area). Representative high magnification images of p-Erk staining from the border zone area of wild type and transgenic mouse hearts 3 days post MI (*D*). Density of p-Erk positive nuclei per mm² in the border zone area (*E*). (WT=81.40 ± 10.10, melusin-TG=125.8 ± 10.66, P=0,0028)

Cell contraction and Ca^{2+} transient amplitude in isolated myocytes 3 days after MI in male mice. (*F*) Mean data of time to peak contraction at 1Hz in wild type sham (n=8, n_{cells}=58), wild type MI (n=7, n_{cells}=62), melusin-TG sham (n=5, n_{cells}=39) and melusin-TG MI (n=4, n_{cells}=38). (*G*) Ca^{2+} transient amplitude in wild type sham (n=8, n_{cells}=22), wild type MI (n=7, n_{cells}=20), melusin-TG sham (n=5, n_{cells}=11) and melusin-TG MI (n=3, n_{cells}=9) (673,5±152,8 in wild type MI vs 233,7±47,42 in melusin-TG MI, P=0,02).

Figure 3:

Melusin overexpression reduces inflammatory infiltration in the infarcted zone. (*A*) Infiltration by CD18 positive inflammatory cells 3 days post MI measured on histological sections of the infarcted zone was significantly reduced in melusin-TG mice compared to WT controls (25.4±3.9 n=15 in wild type vs. 17.2±2.2 n=14 in melusin-TG cells/field, P= 0.0471). Hematoxylin stained histological sections of infarcted hearts three days after MI, revealed that most inflammatory cells have the typical morphology of neutrophil granulocytes (*B* arrowheads). (*C*) Real time PCR analysis at 3 days after MI showed a significantly increased *Pgf* expression in male melusin-TG mice compared to wild type mice (1.94 ± 0.33 in wild type MI vs. melusin-TG MI 6.03 ± 1.47, P= 0,027). (*D*) *Cxcl10* expression, on the other hand, was significantly reduced in melusin-TG mice (23.05±3.06 in wild type MI vs. melusin-TG MI 10.01±1.18, P=0,0073).

Figure 4:

Improved LV remodelling 2 weeks after MI in melusin-TG mice.

(*A*) Heart weight relative to body weight was increased to a similar extent in wild type and melusin-TG mice after MI. However, melusin-TG mice displayed (*B*) reduced LV dilatation (4.65±0.19 in wild type MI vs. 4.04±0.10 in melusin-TG MI, P= 0.007), (*C*) preserved septal wall thickness (0.63±0.05 in wild type MI vs. 0.81±0.05 in melusin-TG MI, P=0.016) and (*D*) improved contractile function compared to wild type mice (22.2±2.2 in wild type MI vs. 28.7±2.1% in melusin-TG MI, P=0.036). (*E*) After MI cardiomyocyte cross sectional area increased significantly in melusin-TG hearts. (*F*) Anf-mRNA (*Nppa*) expression was significantly less increased after MI in melusin-TG compared to wild type mice.

Figure 5:

Melusin overexpression improves cardiomyocyte contractility, reduces collagen deposition and cardiomyocyte apoptosis after MI.

(*A*) Fractional shortening of cardiomyocytes isolated from hearts 14 days after MI was increased in both wild type and melusin-TG mice compared to sham controls. The increase, however, was significantly more pronounced in melusin-TG mice (2-way repeated measures ANOVA, $P<0.05$ for all comparisons). (*B*) SERCA2a protein expression was not significantly affected by MI. (*C*) Interestingly, phosphorylation levels of $TNI^{Ser22/23}$ was reduced in WT, but not in melusin-TG hearts following MI. (*D*) TUNEL staining indicated a significantly lower rate of apoptosis in the remote myocardium of melusin-TG mice. (*E*) Collagen deposition assessed by picrosirius red staining was significantly reduced in the remote myocardium of melusin-TG mice compared to wild type after MI. All data reported are from mice at 14 days after MI.

Figure 1

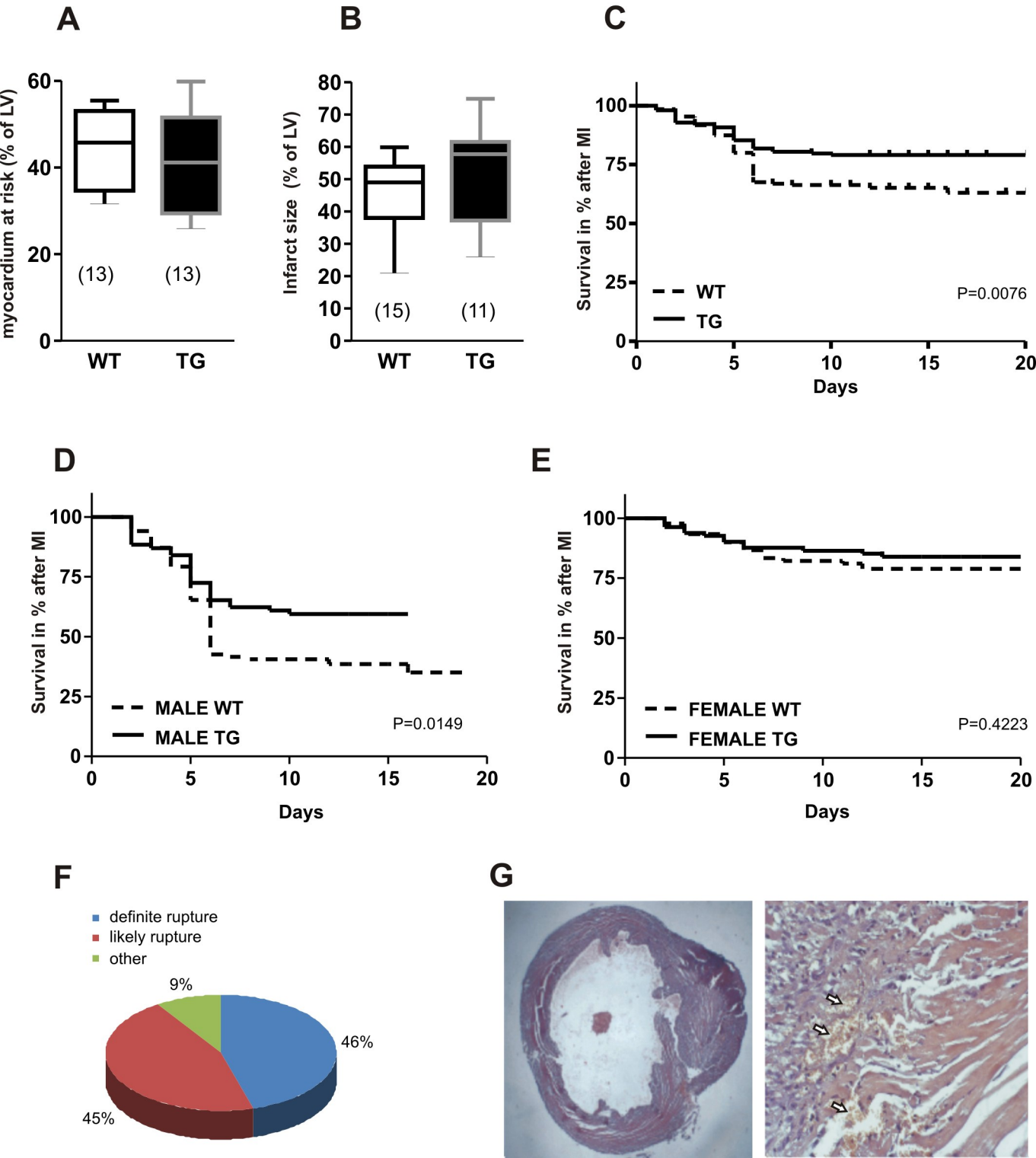
A
B
C
myocardium at risk (% of LV)
60
40
20
0
(13)
(13)
WT
TG
Infarct size (% of LV)
80
70
60
50
40
30
20
10
0
(15)
(11)
WT
TG
Survival in % after MI
100
75
50
25
0
WT
TG
P=0.0076
0
5
10
15
20
Days
D
E
Survival in % after MI
MALE WT
MALE TG
P=0.0149
Days
FEMALE WT
FEMALE TG
P=0.4223
Days
F
G
definite rupture
likely rupture
other
9%
46%
45%

Figure 2

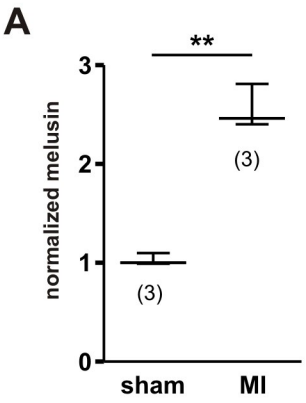
A
**
normalized melusin
3
2
1
0
(3)
(3)
sham
MI

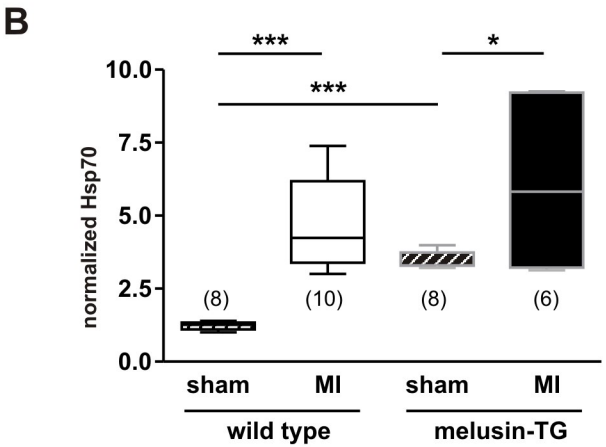
B
***
***
*
normalized Hsp70
10.0
7.5
5.0
2.5
0.0
(8)
(10)
(8)
(6)
sham
MI
sham
MI
wild type
melusin-TG

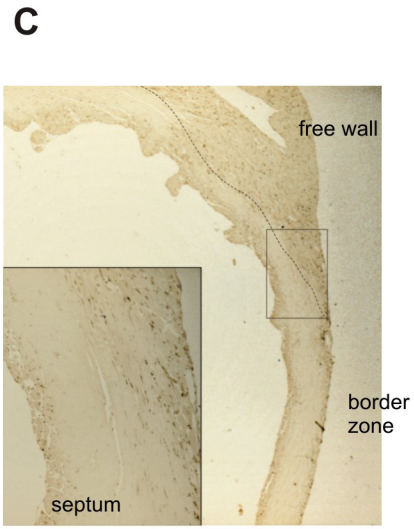
C
free wall
border
zone
septum

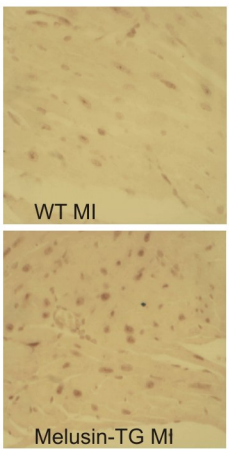
D
WT MI
Melusin-TG MI

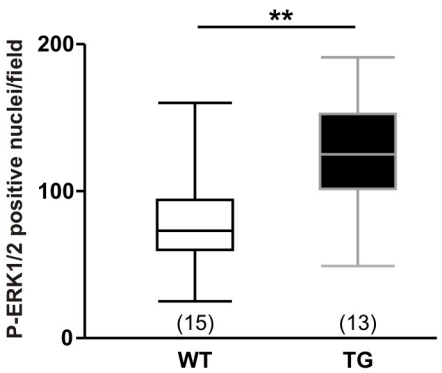
E
**
P-ERK1/2 positive nuclei/field
200
100
0
(15)
(13)
WT
TG

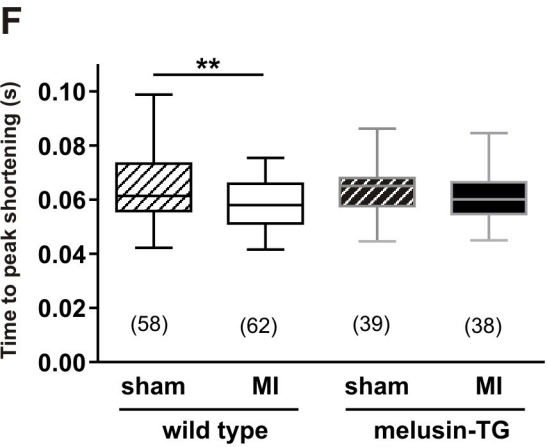
F
**
Time to peak shortening (s)
0.10
0.08
0.06
0.04
0.02
0.00
(58)
(62)
(39)
(38)
sham
MI
sham
MI
wild type
melusin-TG

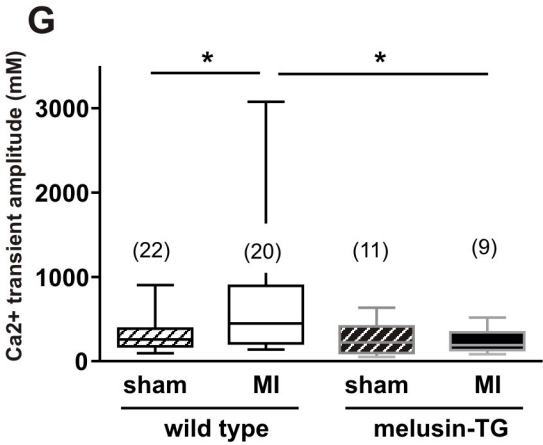
G
*
*
Ca2+ transient amplitude (mM)
3000
2000
1000
0
(22)
(20)
(11)
(9)
sham
MI
sham
MI
wild type
melusin-TG

Figure 3

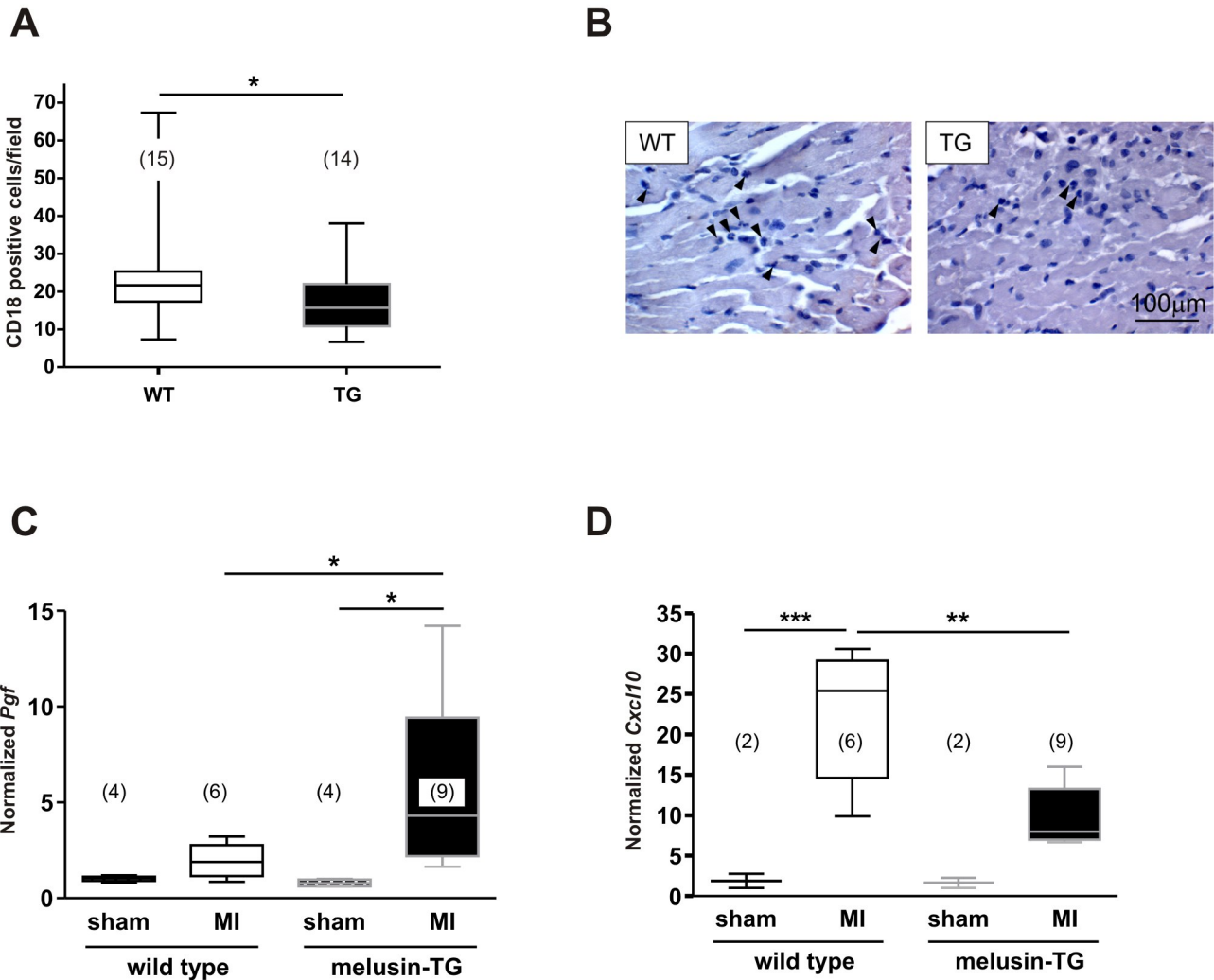
A
B
C
D
CD18 positive cells/field
WT
TG
(15)
(14)
100µm
Normalized Pgf
(4)
(6)
(4)
(9)
sham
MI
sham
MI
wild type
melusin-TG
Normalized Cxcl10
(2)
(6)
(2)
(9)
sham
MI
sham
MI
wild type
melusin-TG

Figure 4

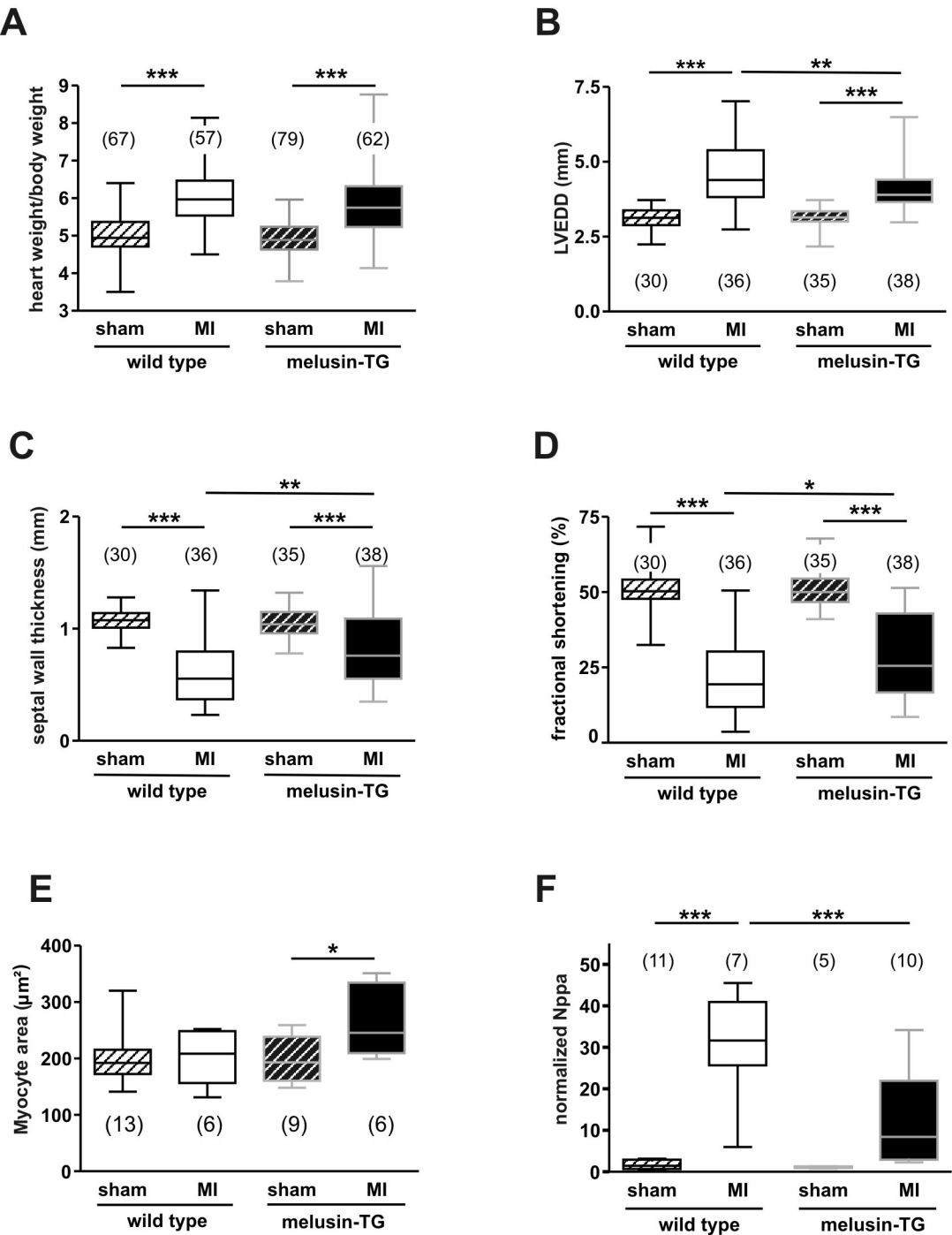
A
heart weight/body weight
***
***
(67)
(57)
(79)
(62)
sham
MI
sham
MI
wild type
melusin-TG
B
LVEDD (mm)
***
**
***
(30)
(36)
(35)
(38)
sham
MI
sham
MI
wild type
melusin-TG
C
septal wall thickness (mm)
**
***
***
(30)
(36)
(35)
(38)
sham
MI
sham
MI
wild type
melusin-TG
D
fractional shortening (%)
*
***
***
(30)
(36)
(35)
(38)
sham
MI
sham
MI
wild type
melusin-TG
E
Myocyte area (μm²)
*
(13)
(6)
(9)
(6)
sham
MI
sham
MI
wild type
melusin-TG
F
normalized Nppa
***
***
(11)
(7)
(5)
(10)
sham
MI
sham
MI
wild type
melusin-TG

Figure 5

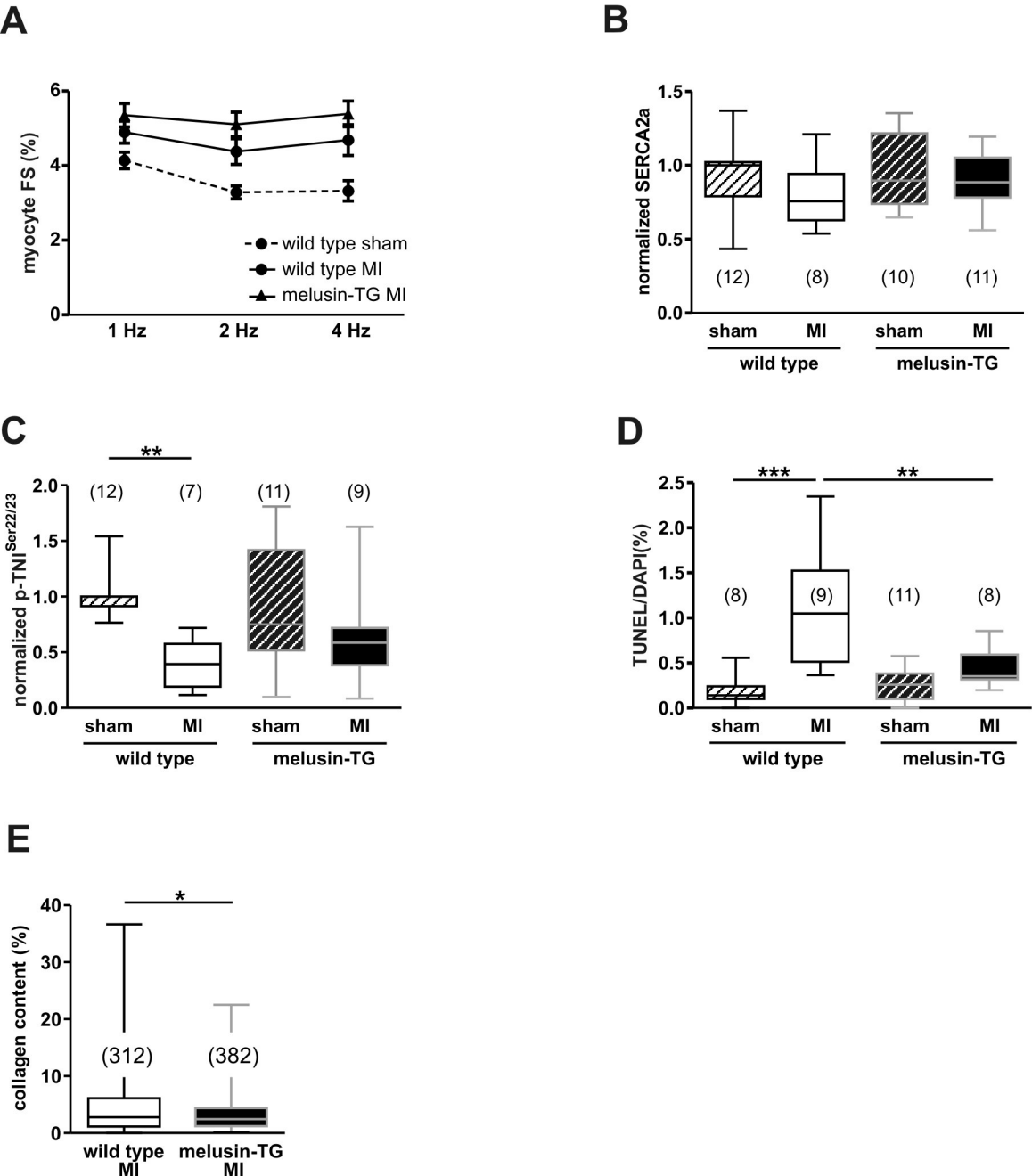
A
myocyte FS (%)
6
4
2
0
1 Hz
2 Hz
4 Hz
wild type sham
wild type MI
melusin-TG MI
B
normalized SERCA2a
1.5
1.0
0.5
0.0
(12)
(8)
(10)
(11)
sham
MI
sham
MI
wild type
melusin-TG
C
**
normalized p-TNI Ser22/23
2.0
1.5
1.0
0.5
0.0
(12)
(7)
(11)
(9)
sham
MI
sham
MI
wild type
melusin-TG
D
***
**
TUNEL/DAPI(%)
2.5
2.0
1.5
1.0
0.5
0.0
(8)
(9)
(11)
(8)
sham
MI
sham
MI
wild type
melusin-TG
E
*
collagen content (%)
40
30
20
10
0
(312)
(382)
wild type MI
melusin-TG MI